Optimal $\mathcal{H}_\infty$ LMI-Based Model Reduction by Moment Matching for Linear Time-Invariant Models

M.F. Shakib[1], G. Scarciotti[2], M. Jungers[3], A.Y. Pogromsky[1], A. Pavlov[4], N. van de Wouw[1,5]

***Abstract*— This paper proposes an approach to model order reduction of stable linear time-invariant models. The proposed approach extends time-domain moment matching by the minimization of the $\mathcal{H}_\infty$ norm of the error dynamics characterizing the difference between the full-order and reduced-order models given fixed interpolation points. The optimal $\mathcal{H}_\infty$ moment matching problem is a constrained optimization problem with bilinear constraints. Introducing a novel numerical procedure, we minimize the approximation error, while respecting the constraints and, thereby, find an suboptimal $\mathcal{H}_\infty$ reduced-order model. The effectiveness of the approach is illustrated in a numerical example.**

I. INTRODUCTION

Model order reduction techniques aim at reducing the complexity of dynamical models. Hereto, many different methods have been proposed in the literature, such as balanced truncation [1], Hankel-norm approximations [5] and the interpolation approach [4]. The moment matching method, see [1], matches the *moments* of the reduced-order model to the *moments* of the full-order model, where moments are the coefficients of the Laurent series expansion of the transfer function at complex interpolation points. Restricting the interpolation points to the imaginary axis makes moment matching particularly useful in applications where an accurate description of the model is required at specific frequencies such as resonance peaks.

In [2], a time-domain interpretation of moment matching is given in terms of matching the steady-state response of the reduced-order model to the steady-state response of the full-order model for a specific class of input signals. This view has led to a new parametrization of reduced-order models that achieve moment matching, which enjoys a parametric freedom that can be exploited to enforce additional properties for the reduced-order model. For example, in [2], this freedom is exploited to achieve moment matching with, amongst others, prescribed pole locations; prescribed zero locations; and an L_2-gain constraint. Besides that, in [10], a similar freedom is used to fit the transient model response in addition to moment matching.

The methods listed above do not exploit the parametric freedom to minimize the $\mathcal{H}_\infty$ norm or $\mathcal{H}_2$ norm of the error dynamics between the reduced-order and full-order model. In that respect, the works in [8], [9] exploit this freedom to minimize the $\mathcal{H}_2$ norm in a constrained optimization problem with bilinear matrix inequality (BMIs) constraints. The authors deal with the BMI constraints using gradient-type methods and convex relaxations of the BMIs into linear matrix inequalities (LMIs). Other related work, not in the scope of *time-domain* moment matching, is the iterative rational Krylov algorithm (IRKA) presented in [6]. IRKA iteratively updates the interpolation points and, thereby, converges to a model with an approximation error in the $\mathcal{H}_2$ norm that satisfies the first-order minimality conditions.

In this paper, for a user-defined set of fixed interpolation points, we exploit the parametric freedom in time-domain moment matching to minimize an upper bound of the approximation error measured in the $\mathcal{H}_\infty$ norm. The interpretation is that the peak error between the frequency response function (FRF) of the full-order and reduced-order models is minimized and that exponential stability is preserved. We first formally pose the optimal $\mathcal{H}_\infty$ moment matching problem as a constrained optimization problem with BMI constraints. After that, we parametrize three sets of models. The first set contains all models that achieve moment matching. The second set is a subset of the first set and characterizes by BMI constraints all models that achieve moment matching with an approximation error (measured in the $\mathcal{H}_\infty$ norm) smaller than a user-defined threshold. The third set is equivalent to the second set, although parametrized differently, which is exploited in the next step to solve the constrained optimization problem.

We present a novel numerical procedure that is based on the family of coordinate-descent algorithms (CDAs), see [12]. A CDA splits the decision variables in the BMIs into two groups such that fixing either one of the groups yields LMIs. Iteratively, CDA fixes one of the groups such that well-established LMI solvers can be used to minimize the constrained optimization problem with LMI constraints. The novel numerical procedure switches between the equivalent model sets two and three, when CDA cannot further decrease the objective of the constrained optimization problem in one of the model sets and returns a suboptimal solution to the optimal $\mathcal{H}_\infty$ moment matching problem. In a numerical example, we illustrate the effectiveness of the proposed approach and show that, for the considered example, the approximation error can be consistently reduced to within a factor two of a fundamental lower bound in [3].

To summarize, this paper presents a model order reduction technique for LTI models that matches the moments of the full-order model and minimizes the approximation error in

[1]Department of Mechanical Engineering, Eindhoven University of Technology, Eindhoven, The Netherlands {m.f.shakib, a.pogromsky,n.v.d.wouw}@tue.nl

[2]Department of Electrical and Electronic Engineering, Imperial College London g.scarciotti@imperial.ac.uk

[3]Université de Lorraine, CNRS, CRAN, Nancy, France marc.jungers@univ-lorraine.fr

[4]Department of Geoscience and Petroleum, NTNU, Trondheim, Norway alexey.pavlov@ntnu.no

[5]Department of Civil, Environmental & Geo- Engineering, University of Minnesota, Minneapolis, U.S.A. n.vandewo@umn.edu

the $\mathcal{H}_\infty$ norm. The contributions of this paper are:

- the problem formulation for the optimal $\mathcal{H}_\infty$ moment matching problem;
- the parametrization of all models that satisfy the constraints of the optimal $\mathcal{H}_\infty$ moment matching problem;
- a novel numerical procedure to find a suboptimal model from the parametrized set.
- a numerical study to investigate properties of the novel numerical procedure.

Notation: The symbols $\mathbb{R}, \mathbb{C}, \mathbb{C}^0$, and $\mathbb{C}^-$ denote the set of real numbers, complex numbers, complex numbers with zero real part and complex numbers with negative real part, respectively. The spectrum of a matrix $A \in \mathbb{R}^{n\times n}$ is denoted by $\sigma(A)$. For a matrix $A \in \mathbb{R}^{n\times n}$, the notation $\mathrm{He}\,(A)$ is short-hand for $A^\top + A$. The set of symmetric positive definite matrices of dimension $n \times n$ is denoted by $\mathbb{S}_n$.

II. PROBLEM SETTING

This section first introduces the considered class of LTI models and defines moments. After that, the optimal $\mathcal{H}_\infty$ moment matching problem is formulated.

A. Moments of LTI models

Consider the class of LTI models described by the following state-space equations:

$$\Sigma(A,B,C): \quad \dot{x} = Ax + Bu, \quad y = Cx, \tag{1}$$

where $x(t) \in \mathbb{R}^n$ is the state, $u(t) \in \mathbb{R}$ is the input, $y(t) \in \mathbb{R}$ is the output, and $A \in \mathbb{R}^{n\times n}, B \in \mathbb{R}^{n\times 1}, C \in \mathbb{R}^{1\times n}$ are the model matrices. Throughout the paper we assume minimality of model (1). The associated transfer function of model (1) is defined as follows:

$$W(s) := C(sI - A)^{-1}B. \tag{2}$$

The 0-moments of model (1) are defined next.

Definition 1 ([2]): Let $s^\star \in \mathbb{C} \setminus \sigma(A)$. The 0-moment of model (1) at $s^\star$ is the complex number $\eta_0^\Sigma(s^\star) := W(s^\star)$.

B. Moment matching problem

Consider the model characterized as follows:

$$\Sigma_\nu(F,G,H): \quad \dot{\xi} = F\xi + Gu, \quad \psi = H\xi \tag{3}$$

with $\xi(t) \in \mathbb{R}^\nu, u(t) \in \mathbb{R}, \psi(t) \in \mathbb{R}$ and $F \in \mathbb{R}^{\nu\times\nu}, G \in \mathbb{R}^{\nu\times 1}$ and $H \in \mathbb{R}^{1\times\nu}$. The transfer function of this model is defined as follows:

$$\Omega(s) := H(sI - F)^{-1}G. \tag{4}$$

In this paper, we focus on matching the zeroth moments and, in addition, minimize the mismatch between $W(j\omega)$ and $\Omega(j\omega)$, for all $\omega \in \mathbb{R}$, measured in the $\mathcal{H}_\infty$ norm, and preserve stability properties of the full-order model.

Assumption 1: The matrix A of the LTI model (1) is Hurwitz, i.e., $\sigma(A) \in \mathbb{C}^-$.

Definition 2 ([11]): Consider model (1) with transfer function $W(s) \in \mathbb{C}$ in (2) and suppose that Assumption 1 holds. The $\mathcal{H}_\infty$ norm of the transfer function $W(s)$, denoted by $\|W(s)\|_\infty$, is defined as follows:

$$\|W(s)\|_\infty := \sup_{\omega\in[0,\infty)} |W(j\omega)|. \tag{5}$$

Now, we are in a position to formally pose the optimal $\mathcal{H}_\infty$ moment matching problem.

Problem 1: Consider the full-order model (1) and any given matrix $S \in \mathbb{R}^{\nu\times\nu}$ with simple eigenvalues $\sigma(S) = \{s_1, \ldots, s_\nu\}$ on the imaginary axis. Suppose Assumption 1 holds. Consider the reduced-order model (3) characterized by F, G and H. The optimal $\mathcal{H}_\infty$ model matching problem is the following constrained optimization problem:

$$\min_{F,G,H,\gamma} \ \gamma \quad \text{subject to} \tag{6a}$$

$$\|W(s) - \Omega(s)\|_\infty < \gamma, \tag{6b}$$

$$F \text{ is Hurwitz}, \tag{6c}$$

$$\eta_0^\Sigma(s_i) = \eta_0^{\Sigma_\nu}(s_i), \text{ for all } i = 1, \ldots, \nu. \tag{6d}$$

Constraint (6b) minimizes the peak error between $W(j\omega)$ and $\Omega(j\omega)$, for all $\omega \in \mathbb{R}$. Constraint (6c) ensures that the reduced-order model preserves the exponential stability property of the full-order model. Constraint (6d) matches the zeroth moments $\eta_0^{\Sigma_\nu}$ of the reduced-order model to the zeroth moments of the full-order model η_0^Σ. One could interpret the minimum in this problem as an infimum, for which the numerical solver should return a sufficiently accurate result. The next section proposes the solution to Problem 1.

III. SOLUTION TO THE OPTIMAL $\mathcal{H}_\infty$ MOMENT MATCHING PROBLEM

A. Conceptual description of the approach

The solution strategy for Problem 1 works as follows. In the first step, according to the framework of [2], a set of reduced-order models is constructed such that constraint (6d) is satisfied, i.e., the moments are matched. This set of models enjoys a specific parametric freedom, which we exploit in the second step to present two sets of models that satisfy all constraints of Problem 1 for a given γ. In the third and last step, we present a numerical procedure to minimize γ such that the set of models that satisfies all constraints of Problem 1 is non-empty, which in turn allows to select F, G and H. The resulting reduced-order model then satisfies all constraints of Problem 1 for the minimized γ.

B. Set of reduced-order LTI models satisfying constraint (6d) of Problem 1

The set of models that satisfies the constraint (6d) of Problem 1 is presented in the following theorem and is parametrized by the matrix $G \in \mathbb{R}^{\nu\times 1}$.

Theorem 1 ([2]): Consider the full-order model (1) characterized by the matrices A, B and C, the matrix $S \in \mathbb{R}^{\nu\times\nu}$ as given in Problem 1, and any matrix $L \in \mathbb{R}^{1\times\nu}$ such that the pair (S, L) is observable. For any $G \in \mathcal{G}$ with

$$\mathcal{G} := \left\{ G \in \mathbb{R}^{\nu\times 1} \,:\, \sigma(S) \cap \sigma(S - GL) = \emptyset \right\}, \tag{8}$$

the reduced-order model (3) with matrices

$$F := S - GL, \quad H := C\Pi, \tag{9}$$

$$\mathcal{L}_\gamma^I(\mathcal{X},G) := \begin{bmatrix} A^\top\mathcal{X}_1+\mathcal{X}_1A & A^\top\mathcal{X}_3+\mathcal{X}_3S-\mathcal{X}_3GL & \mathcal{X}_1B+\mathcal{X}_3G & C^\top \\ * & S^\top\mathcal{X}_2-L^\top G^\top\mathcal{X}_2+\mathcal{X}_2S-\mathcal{X}_2GL & \mathcal{X}_3^\top B+\mathcal{X}_2G & -H^\top \\ * & * & -\gamma & 0 \\ * & * & * & -\gamma \end{bmatrix} \tag{7}$$

where $\Pi \in \mathbb{R}^{n\times\nu}$ is the unique solution to the equation

$$\Pi S = A\Pi + BL, \tag{10}$$

interpolates the moments of the full-order model (1) at the eigenvalues of S. Furthermore, the set $\mathcal{G}$ characterizes *all* the reduced-order models of order ν that interpolate the moments of the full-order model (1) at the eigenvalues of S.

The set $\mathcal{G}$ presented in Theorem 1 contains all the models that satisfy constraint (6d). In the next section, we characterize a subset of $\mathcal{G}$ that, in addition to constraint (6d), also satisfies the two constraints (6b) and (6c) for a fixed γ.

C. Set of reduced-order LTI models satisfying all constraints of Problem 1

We use matrix inequalities to characterize the set of models that satisfy all the constraints of Problem 1. In particular, we use the so-called Bounded-Real Lemma.

Lemma 1 ([11]): Consider an LTI model characterized by $\mathcal{A},\mathcal{B},\mathcal{C}$. For any $\gamma>0$,

$$\sigma(\mathcal{A}) \in \mathbb{C}^- \quad \text{and} \quad \left\|\mathcal{C}(sI-\mathcal{A})^{-1}\mathcal{B}\right\|_\infty < \gamma$$

hold true if and only if the following set of LMIs is feasible

$$\begin{bmatrix} \mathcal{A}^\top\mathcal{X}+\mathcal{X}\mathcal{A} & \mathcal{X}\mathcal{B} & \mathcal{C}^\top \\ \mathcal{B}^\top\mathcal{X} & -\gamma I & 0 \\ \mathcal{C} & 0 & -\gamma I \end{bmatrix} \prec 0, \quad \mathcal{X}\succ 0. \tag{11}$$

Using Lemma 1, we can construct the first set of models in which the following partition of $\mathcal{X}$ is employed:

$$\mathcal{X} := \begin{bmatrix} \mathcal{X}_1 & \mathcal{X}_3 \\ \mathcal{X}_3^\top & \mathcal{X}_2 \end{bmatrix}, \mathcal{X}_1 \in \mathbb{R}^{n\times n}, \mathcal{X}_2 \in \mathbb{R}^{\nu\times\nu}, \mathcal{X}_3 \in \mathbb{R}^{n\times\nu}.$$

Theorem 2: Consider the full-order model described by the triple (A,B,C) in (1) and the set of reduced-order models described by (F,H) in (9) and characterized by $G \in \mathcal{G}$ in Theorem 1. Given a fixed $\gamma > 0$, for any $G \in \mathcal{G}_\gamma^I \subset \mathcal{G}$ with

$$\mathcal{G}_\gamma^I := \left\{G \in \mathbb{R}^{\nu\times 1} : \exists \mathcal{X} \in \mathbb{S}_{n+\nu} : \mathcal{L}_\gamma^I(\mathcal{X},G) \prec 0\right\}, \tag{12}$$

the constraints (6b) - (6d) of Problem 1 are satisfied, where $\mathcal{L}_\gamma^I(\mathcal{X},G)$ is defined in (7). Furthermore, the set of reduced-order models (3) characterized by $G \in \mathcal{G}_\gamma^I$ contains *all* models that satisfy constraints (6b) - (6d) of Problem 1. Moreover, if the full-order model characterized by A,B,C is balanced[1] with Hankel singular values[2] $h_1 \geq \ldots \geq h_\nu \geq h_{\nu+1} \geq \ldots \geq h_n$, then the set $\mathcal{G}_\gamma^I$ is empty for $\gamma < h_{\nu+1}$.

Proof: The proof is omitted for brevity. ■

Notice that the matrix $\mathcal{L}_\gamma^I(\mathcal{X},G)$ in (7) contains products between G and $\mathcal{X}_2,\mathcal{X}_3$. In the scope of minimizing γ while respecting the constraints of Problem 1, a formulation that does not contain such products is favorable. Hereto, consider the set $\mathcal{G}_\gamma^{II}$ defined as follows:

$$\begin{aligned}\mathcal{G}_\gamma^{II} := \big\{G \in \mathbb{R}^{\nu\times 1} : \exists \mathcal{X} \in \mathbb{S}_{n+\nu}, \\ \exists N \in \mathbb{R}^{n+2\nu+2\times n} : \mathcal{L}_\gamma^{II}(\mathcal{X},N,G) \prec 0\big\},\end{aligned} \tag{13}$$

where $\mathcal{L}_\gamma^{II}(\mathcal{X},N,G)$ is defined as follows:

$$\mathcal{L}_\gamma^{II}(\mathcal{X},N,G) := \begin{bmatrix} M_0 & M_1 \\ M_1^\top & 0_{\nu\times\nu} \end{bmatrix} + \text{He}\left(N\begin{bmatrix} M_2^\top & -I_\nu \end{bmatrix}\right)$$

with

$$M_0 = \begin{bmatrix} A^\top\mathcal{X}_1+\mathcal{X}_1A & A^\top\mathcal{X}_3+\mathcal{X}_3S & \mathcal{X}_1B & C^\top \\ * & S^\top\mathcal{X}_2+\mathcal{X}_2S & \mathcal{X}_3^\top B & -H^\top \\ * & * & -\gamma & 0 \\ * & * & * & -\gamma \end{bmatrix},$$

$$M_1^\top = \begin{bmatrix} \mathcal{X}_3^\top & \mathcal{X}_2 & 0_{\nu\times 1} & 0_{\nu\times 1} \end{bmatrix},$$

$$M_2^\top = \begin{bmatrix} 0_{\nu\times n} & -GL & G & 0_{\nu\times 1} \end{bmatrix}.$$

The following theorem shows equivalence between the sets $\mathcal{G}_\gamma^I$ in (12) and $\mathcal{G}_\gamma^{II}$ in (13).

Theorem 3: The candidate $G \in \mathcal{G}_\gamma^I$ if and only if $G \in \mathcal{G}_\gamma^{II}$, where the set $\mathcal{G}_\gamma^I$ is defined in (12) and the set $\mathcal{G}_\gamma^{II}$ in (13).

Proof: The proof is omitted for brevity. ■

The matrix $\mathcal{L}_\gamma^{II}(\mathcal{X},N,G)$ does not contain products between $\mathcal{X}$ and G, but instead contains a product between N and G. The availability of the two equivalent sets $\mathcal{G}_\gamma^I$ and $\mathcal{G}_\gamma^{II}$ is exploited in the numerical procedure to solve Problem 1, as presented in the next section.

Remark 1: The sets $\mathcal{G}_\gamma^I$ and $\mathcal{G}_\gamma^{II}$ described in Theorems 2 and 3 contain no conservatism, i.e., for a given γ, *all* models with state dimension ν that satisfy the constraints (6b) - (6d) of Problem 1 are characterized by each of these sets.

Remark 2: If the full-order model is balanced, then Theorem 2 provides a lower bound for γ in constraint (6b), namely

$$\|W(s)-\Omega(s)\|_\infty \geq h_{\nu+1}, \tag{14}$$

where $h_{\nu+1}$ the $(\nu+1)^{\text{th}}$ largest Hankel singular value of the full-order model. We note that (14) also holds without constraint (6d) of Problem 1. Therefore, it is likely that this bound is conservative in the scope of moment matching, i.e., respecting constraint (6d) of Problem 1.

D. Numerical procedure for solving the $\mathcal{H}_\infty$ moment matching problem

In the previous section, we have formulated sets $\mathcal{G}_\gamma^I$ and $\mathcal{G}_\gamma^{II}$ that parametrize all models that satisfy the constraints of Problem (6) for a given $\gamma > 0$. In this section, we propose a numerical procedure to minimize γ, while respecting the constraints characterizing the sets $\mathcal{G}_\gamma^I$ and $\mathcal{G}_\gamma^{II}$.

It is well-known that $\mathcal{H}_\infty$ model order reduction problems lead to bilinear matrix inequalities (BMIs) constraints [7], [3]. More particularly, as stated in [3], $\mathcal{H}_\infty$ model order

[1]A model is called balanced if its observability and controllability Gramians are equal and diagonal.

[2]The Hankel singular values of a balanced model are the diagonal entries of the Gramian matrix.

reduction can be regarded as a special case of the reduced-order $\mathcal{H}_\infty$ controller synthesis problem, for which no LMI formulation exists yet. In that respect, the results of this paper are no exception, as the constraints in $\mathcal{G}_\gamma^I$ and $\mathcal{G}_\gamma^{II}$ are BMIs due to the products between the variables G and $\mathcal{X}_2, \mathcal{X}_3$ in $\mathcal{L}_\gamma^I(\mathcal{X}, G)$ and the products between N and G in $\mathcal{L}_\gamma^{II}(\mathcal{X}, N, G)$. Solving optimization problems with BMI constraints is a challenging task for which it is difficult to guarantee convergence towards the global optimum [12].

One method to solve an optimization problem with BMI constraints is the coordinate-descent algorithm (CDA) [12]. This algorithm splits the bilinear variables into two sets such that fixing either one of the two sets turns the BMI constraints into LMI constraints. CDA iteratively fixes one set of variables and optimizes γ for the other, for example, by a bi-section search over γ. Even without a formal proof of convergence, CDA works well in practice and guarantees a non-increasing sequence of γ over the iterations [12].

Let us focus on the constraints in $\mathcal{G}_\gamma^I$ first, for which the CDA is listed in Algorithm 1. Here, the partitioning of $\mathcal{X}$ in (**??**) is used and the iteration index is denoted in the superscript. In Step 3 of this algorithm, for a given, fixed $G \in \mathcal{G}_\gamma^I$, the corresponding constrained optimization problem is solved, where the constraints are LMIs in the variable $\mathcal{X}$. This step is nothing more than computing a tight upper bound for $\|W(s) - \Omega(s)\|_\infty$. After that, in Step 4, for the computed $\mathcal{X}_2, \mathcal{X}_3$ in Step 3, the corresponding constrained optimization problem is solved, where the constraints are again LMIs, but now in the variables $\mathcal{X}_1$ and G. This step aims at finding a G such that $\|W(s) - \Omega(s)\|_\infty$ is decreased for the given $\mathcal{X}_2, \mathcal{X}_3$. To launch this algorithm, an initial $G^{[0]}$ is required that is inside the feasible set of the constraints, i.e., $G^{[0]} \in \mathcal{G}_\gamma^I$. In the next section, we present a method to construct such initial $G^{[0]}$. Note that for CDAs, the sequence $\gamma^{[1]}, \gamma^{[2]}, \ldots$ is non-increasing, as the solution to the previous iteration is a feasible starting point of each optimization problem in Steps 3 and 4.

Analogously to Algorithm 1, Algorithm 2 presents the CDA for iterations in $\mathcal{L}_\gamma^{II}(\mathcal{X}, N, G)$. In Step 3, the variables G is fixed, whereas in Step 4, the variable N is fixed.

The introduction of two CDAs enables switching between Algorithms 1 and 2, when the respective CDA cannot decrease γ anymore. For example, suppose that Algorithm 1 is performed and returned $G_I \in \mathcal{G}_\gamma^I$. Then, the idea is to use $G_I \in \mathcal{G}_\gamma^I$ as a starting point for Algorithm 2, i.e., $G_{II}^{[0]} = G_I$, and run Algorithm 2. Similarly, after running Algorithm 2 and obtaining $G_{II} \in \mathcal{G}_\gamma^{II}$, the idea is to use $G_I^{[0]} = G_{II}$ to launch Algorithm 1. Note that this switching is possible thanks to the equivalence between sets $\mathcal{G}_\gamma^I$ and $\mathcal{G}_\gamma^{II}$, as presented in Theorem 3. The resulting numerical procedure is formalized in Algorithm 3, where we choose to start with the CDA in Algorithm 2, as this CDA appears to converge quicker than the one in Algorithm 1. Studying properties of Algorithm 3, e.g., convergence and robustness with respect to the starting point, is a topic for future work. Therefore, we cannot guarantee that this algorithm returns an optimal model and we call the found model suboptimal. A preliminary numerical study is presented in Section IV.

E. Finding an initial $G^{[0]}$

In order to launch Algorithm 3, an initial $G^{[0]} \in \mathcal{G}_{\gamma^{[0]}}^{II}$ and $\gamma^{[0]}$ is required. Hereto, consider the result of Theorem 1, which states that any reduced-order model characterized by $G \in \mathcal{G}$ satisfies constraint (6d). By observability of the pair (S, L), which is assumed in Theorem 1, the eigenvalues of F in (9) can be placed at any desired location by full-state feedback. Placing the eigenvalues of F in the open complex left-half plane, i.e., $\sigma(F) \in \mathbb{C}^-$, yields a model

Algorithm 1 CDA for $\mathcal{L}_\gamma^I(\mathcal{X}, G)$

Input: Model matrices A, B, C of full-order model (1), matrices S, L as in Theorem 1, H as in (9), any vector $G^{[0]} \in \mathcal{G}_{\gamma^{[0]}}^I$, $\gamma^{[0]} > 0$, and an accuracy threshold $\epsilon > 0$.

1: Iteration index $i = 1$.
2: **while** $(\gamma^{[i-1]} - \gamma^{[i]})/\gamma^{[i]} \geq \epsilon$ **do**
3: Solve the optimization problem

$$\left(\cdot, \mathcal{X}_2^{[i]}, \mathcal{X}_3^{[i]}, \cdot\right) = \underset{\mathcal{X}_1, \mathcal{X}_2, \mathcal{X}_3, \gamma}{\arg\min}\ \gamma \quad \text{subject to}$$
$$\mathcal{L}_\gamma^I\left(\begin{bmatrix} \mathcal{X}_1 & \mathcal{X}_3 \\ * & \mathcal{X}_2 \end{bmatrix}, G^{[i-1]}\right) \prec 0, \begin{bmatrix} \mathcal{X}_1 & \mathcal{X}_3 \\ * & \mathcal{X}_2 \end{bmatrix} \succ 0.$$

4: Solve the optimization problem

$$\left(\cdot, G^{[i]}, \gamma^{[i]}\right) = \underset{\mathcal{X}_1, G, \gamma}{\arg\min}\, \gamma \quad \text{subject to}$$
$$\mathcal{L}_\gamma^I\left(\begin{bmatrix} \mathcal{X}_1 & \mathcal{X}_3^{[i]} \\ * & \mathcal{X}_2^{[i]} \end{bmatrix}, G\right) \prec 0, \begin{bmatrix} \mathcal{X}_1 & \mathcal{X}_3^{[i]} \\ * & \mathcal{X}_2^{[i]} \end{bmatrix} \succ 0.$$

5: Update $i = i + 1$.
6: **end**

Output: Matrix $G_I = G^{[i-1]}$ and scalar $\gamma_I = \gamma^{[i-1]}$.

Algorithm 2 CDA for $\mathcal{L}_\gamma^{II}(\mathcal{X}, N, G)$

Input: Model matrices A, B, C of full-order model (1), matrices S, L as in Theorem 1, H as in (9), any vector $G^{[0]} \in \mathcal{G}_{\gamma^{[0]}}^I$, $\gamma^{[0]} > 0$, and an accuracy threshold $\epsilon > 0$.

1: Iteration index $i = 1$.
2: **while** $(\gamma^{[i-1]} - \gamma^{[i]})/\gamma^{[i]} \geq \epsilon$ **do**
3: Solve the optimization problem

$$\left(\cdot, N^{[i]}, \cdot\right) = \underset{\mathcal{X}, N, \gamma}{\arg\min}\, \gamma$$
$$\text{subject to } \mathcal{L}_\gamma^{II}(\mathcal{X}, N, G^{[i-1]}) \prec 0, \mathcal{X} \succ 0.$$

4: Solve the optimization problem

$$\left(\cdot, G^{[i]}, \gamma^{[i]}\right) = \underset{\mathcal{X}, G, \gamma}{\arg\min}\, \gamma$$
$$\text{subject to } \mathcal{L}_\gamma^{II}(\mathcal{X}, N^{[i]}, G) \prec 0, \mathcal{X} \succ 0.$$

5: Update $i = i + 1$.
6: **end**

Output: Matrix $G_{II} = G^{[i-1]}$ and scalar $\gamma_{II} = \gamma^{[i-1]}$.

Algorithm 3 Combination of CDAs

Input: Model matrices A, B, C of full-order model (1), matrices S, L as in Theorem 1, H as in (9), any vector $G_{II}^{[0]} \in \mathcal{G}_{\gamma^{[0]}}^{II}$, $\gamma^{[0]} > 0$, and an accuracy threshold $\epsilon > 0$.

1: Set iteration index $k = 1$.
2: **while** $(\gamma^{[k-1]} - \gamma^{[k]})/\gamma^{[k]} \geq \epsilon$, **do**
3: Obtain $G_{II}^{[k]} = G_{II}$ and $\gamma^{[k]} = \gamma_{II}$ by running Algorithm 2 starting from $G_I^{[k-1]}$.
4: Set $k = k + 1$.
5: Obtain $G_I^{[k]} = G_I$ and $\gamma^{[k]} = \gamma_I$ by running Algorithm 1 starting from $G_{II}^{[k-1]}$.
6: Update $k = k + 1$.
7: **end**

Output: Matrix $G = G_I^{[k]}$ and scalar $\gamma = \gamma^{[k]}$.

that satisfies constraint (6c). Since $\sigma(F) \in \mathbb{C}^-$, the constraint $\sigma(F) \cap \sigma(S) = \emptyset$ in $\mathcal{G}$ is trivially satisfied and the constraint (6b) is also satisfied for some $\gamma^\star > 0$. Therefore, any $G^{[0]}$ that renders $\sigma(F) \in \mathbb{C}^-$ is a valid starting point with $\gamma^{[0]} = \gamma^\star$. In the examples presented in the next section, we select the locations for the eigenvalues of $F = S - G_I^{[0]} L$ to be a subset of the eigenvalues of A of the full-order model, which is shown to work well in practice.

IV. Illustrative Example

This section presents an example that shows the effectiveness of our approach. The considered full-order model with transfer function $W(s)$ has state dimension $n = 20$ and is already balanced. We apply the methods presented in this paper to find reduced-order models with state dimensions $\nu = 2, 4$ and 6 and corresponding transfer functions $\Omega_\nu(s)$.

First, we select interpolation points $s_i, i = 1, \ldots, 6$, on the imaginary axis, as in Problem 1. Hereto, consider the FRF of the full-order model depicted in Figure 1. Firstly, we would like to match the moment that corresponds to the largest resonance peak at $f_1 = 2.24$ Hz. Secondly, we would like to match the moment that corresponds to the second largest resonance peak at $f_2 = 0.82$ Hz. Lastly, to capture the low-frequency behavior, we match the moment that corresponds to $f_3 = 0.01$ Hz. The frequencies f_1, f_2, f_3 are marked with a cross in Figure 1. We select the interpolation points $s_i \in \{\pm j \cdot 2\pi f_1, \pm j \cdot 2\pi f_2, \pm j \cdot 2\pi f_3\}$. For the $\nu = 2$-dimensional reduced-order model, we only match $s_{1,2}$ corresponding to the largest resonance peak, for the $\nu = 4$-dimensional model, we match $s_{1,2,3,4}$ corresponding to the two largest resonance peaks, and for the $\nu = 6$-dimensional model, we match all $s_i, i = 1, \ldots, 6$, corresponding to frequencies f_1, f_2, and f_3. For each frequency, we define the matrix

$$\Xi_k = \begin{bmatrix} 0 & 2\pi \cdot f_k \\ -2\pi \cdot f_k & 0 \end{bmatrix}, L_k = \begin{bmatrix} 1 & 0 \end{bmatrix}.$$

Under these choices, the conditions in Theorem 1 for the pair (S, L) are satisfied for

$$S := \text{blockdiag}(\Xi_1, \ldots, \Xi_{\nu/2}), L := \begin{bmatrix} L_1 & \ldots & L_{\nu/2} \end{bmatrix}.$$

Next, for each case of ν, we solve equation (10) for the unique Π and define F and H according to (9), which defines the set $\mathcal{G}$. From the set $\mathcal{G}$, we select an initial $G^{[0]} \in \mathcal{G}_{\gamma^\star}^I$ by pole placement. Hereto, we choose the placement locations as a subset of the eigenvalues of A, namely: $p_1 = \{-0.337 \pm 14.053j\}, p_2 = \{-0.798 \pm 5.2129j\}, p_3 = \{-0.225, -10.490\}$. To assess sensitivity to the pole locations of the initial reduced-order model, we run Algorithm 3 multiple times for each ν, each time starting with different initial locations as indicated in Table I, where for 'Random', the pole locations are drawn from a normal distribution and mirrored to $\mathbb{C}^-$. The approximation error in the $\mathcal{H}_\infty$ norm of the initial model with $G^{[0]}$ is included in Table I in the column γ_{init}. The optimization problem (6a) in Problem 1 is solved using SeDuMi in Matlab.

TABLE I: Considered studies.

Study	ν	$h_{\nu+1}$	$\sigma(S - G^{[0]}L)$	γ_{init}	γ_{final}
1	2	0.777	p_1	1.250	1.195
2			p_2	44.084	1.218
3			p_3	21.348	1.225
4	4	0.321	p_1 and p_2	1.244	0.557
5			p_1 and p_3	11.628	0.550
6			p_2 and p_3	16.236	0.557
7	6	0.038	p_1, p_2 and p_3	0.797	0.066
8			Random	14.943	0.066

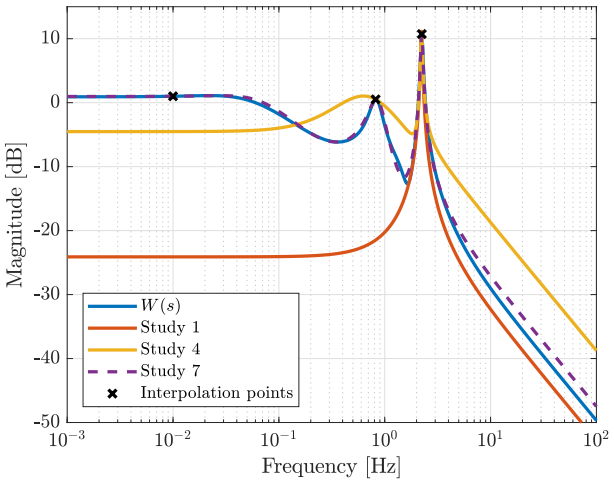

Fig. 1: Bode magnitude plot of the full-order model $W(s)$ and the reduced-order model $\Omega(s)$ of Studies $1, 4$ and 7.

Figure 1 depicts the magnitude of the FRF $W(j\omega)$ and the magnitude of the FRFs $\Omega_\nu(j\omega)$ for studies $1, 4, 7$. The FRFs obtained in Studies 2 and 3, Studies 5 and 6, and Study 8 are left out of this figure as they are similar to the FRFs in Study 1, Study 4 and Study 7, respectively. It can be seen that for any ν, the error $|W(j\omega) - \Omega_\nu(j\omega)|$ is 0 at the corresponding interpolation frequencies f_1, f_2, and f_3, i.e., for $\nu = 2$ only f_1, etc. This is a characteristic property of moment matching. Secondly, it can be observed that increasing ν yields a reduced-order model that significantly more accurately matches the FRF of the full-order model.

The approximation error after application of Algorithm 3 is included in Table I in the column γ_{final}. Firstly, as expected, a larger ν allows for a reduced approximation error thanks

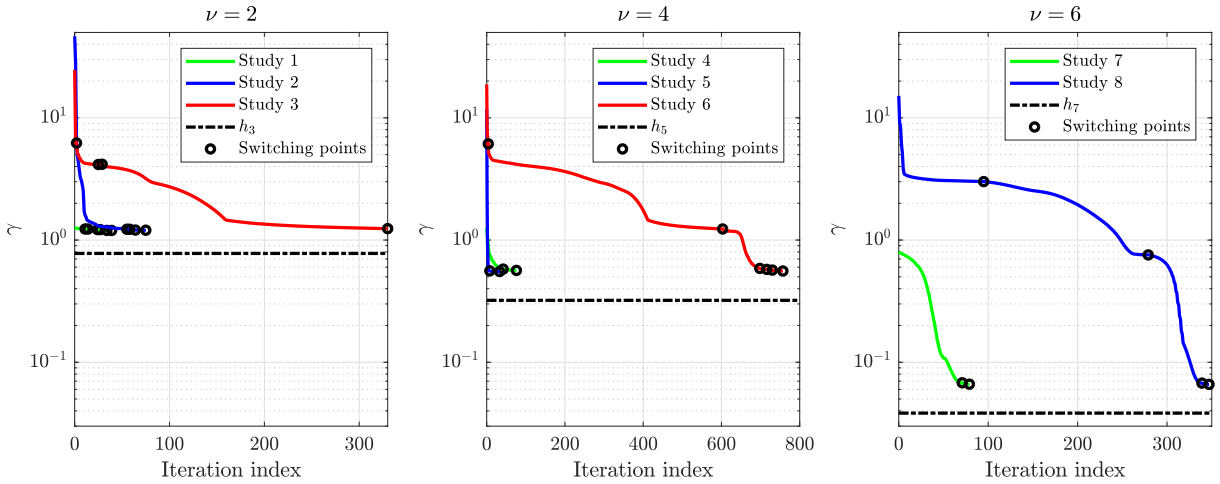

Fig. 2: Iteration history of γ for the considered studies in Table I (left: $\nu = 2$, middle: $\nu = 4$, right: $\nu = 6$). The dashed black line corresponds to the lower bound based on the Hankel singular values. The circles correspond to switches in Algorithm 3 between Algorithms 1 and 2.

to the increased model flexibility. Secondly, it can be seen that in all cases, the approximation error is significantly reduced from γ_{init} to γ_{final}; in all cases within a factor 2 of the fundamental lower bound $h_{\nu+1}$, i.e., $\gamma_{\text{final}} < 2 \cdot h_{\nu+1}$. Thirdly, it can be seen that in all considered cases, Algorithm 3 is robust for the initial starting $G^{[0]}$, as it converges to the same level of approximation error in terms of γ for any of the tested initial starting $G^{[0]}$. Given the fact that the approximation error is relatively close to the conservative lower bound in (14) and given the robustness of Algorithm 3 against the initial starting $G^{[0]}$, we conclude that the proposed method is effective. Nevertheless, studying the properties of Algorithm 3 in terms of convergence and robustness for the starting point remains a topic for future work. A second conclusion is that placing the poles of the initial reduced-order model to a subset of $\sigma(A)$ is also effective. For example, placing the poles of the initial reduced-order model at p_1 captures the largest resonance peak.

The iteration history for γ is depicted in Figure 2 for each ν. Based on this figure, we would like to highlight two important observations for the considered cases. Firstly, if we have a reasonable initial $G^{[0]}$, then the algorithm converges within a 100 iterations, for which the computational time is approximately 10 minutes (on an Intel Core i7-7700HQ, 2.8 GHz processor). Secondly, the switching nature of Algorithm 3 helps to reduce γ. For example, in Study 8, several switches are made between the CDAs in Algorithms 1 and 2, when the corresponding algorithm failed to reduced γ further. Thus, in the considered cases, Algorithm 3 avoids getting stuck prematurely at suboptimal reduced-order models by switching between the different CDAs.

V. CONCLUSIONS

This paper presents an optimal $\mathcal{H}_\infty$ model order reduction by moment matching for exponentially stable LTI models. The considered optimal $\mathcal{H}_\infty$ moment matching problem enforces exponential stability and minimizes the approximation error measured in the $\mathcal{H}_\infty$ norm in addition to matching the zeroth moments. The proposed approach exploits the freedom that time-domain moment matching enjoys to characterize sets of all reduced-order models that solve the optimal $\mathcal{H}_\infty$ moment matching problem for a given accuracy level. Based on these sets of models, a numerical procedure that is an adapted version of the coordinate-descent method, is presented that minimizes the approximation error numerically and, thereby, solves the $\mathcal{H}_\infty$ moment matching problem. Future work aims at analyzing properties of the numerical procedure. In an example, we illustrated the effectiveness and benefits of the proposed approach.

REFERENCES

[1] A.C. Antoulas. *Approximation of large-scale dynamical systems*. SIAM, 2005.

[2] A. Astolfi. Model reduction by moment matching for linear and nonlinear systems. *IEEE Transactions on Automatic Control*, 55(10):2321–2336, 2010.

[3] Y. Ebihara and T. Hagiwara. On $\mathcal{H}_\infty$ model reduction using LMIs. *IEEE Transactions on Automatic Control*, 49(7):1187–1191, 2004.

[4] K. Gallivan, A. Vandendorpe, and P. Van Dooren. Sylvester equations and projection-based model reduction. *Journal of Computational and Applied Mathematics*, 162(1):213–229, 2004.

[5] K. Glover. All optimal hankel-norm approximations of linear multivariable systems and their L^∞-error bounds. *International journal of control*, 39(6):1115–1193, 1984.

[6] S. Gugercin, A.C. Antoulas, and C. Beattie. $\mathcal{H}_2$ model reduction for large-scale linear dynamical systems. *SIAM journal on matrix analysis and applications*, 30(2):609–638, 2008.

[7] A. Helmersson. Model reduction using LMIs. In *Proceedings of the Conference on Decision and Control*, 1994.

[8] I. Necoara and T.C. Ionescu. Optimal H_2 moment matching-based model reduction for linear systems by (non) convex optimization. *arXiv preprint arXiv:1811.07409*, 2018.

[9] I. Necoara and T.C. Ionescu. Parameter selection for best H_2 moment matching-based model approximation through gradient optimization. In *2019 18th European Control Conference (ECC)*, pages 2301–2306. IEEE, 2019.

[10] G. Scarciotti, Z.P. Jiang, and A. Astolfi. Data-driven constrained optimal model reduction. *European Journal of Control*, 53:68–78, 2020.

[11] C.W. Scherer. *The Riccati inequality and state-space H_∞-optimal control*. PhD thesis, Citeseer, 1990.

[12] E. Simon, P. R-Ayerbe, C. Stoica, D. Dumur, and V. Wertz. LMIs-based coordinate descent method for solving BMIs in control design. *IFAC Proceedings Volumes*, 44(1):10180–10186, 2011.